

Spin transport in higher n -acene molecules

R. Pilevarshahri¹, I. Rungger², T. Archer², S. Sanvito² and
N. Shahtahmasebi¹

1)Physics Dep., Faculty of Sciences, Ferdowsi University of Mashhad, Iran 2)School
of Physics and CRANN, Trinity College, Dublin 2, Ireland

E-mail: pilevarr@tcd.ie, runggeri@tcd.ie

Abstract. We investigate the spin transport properties of molecules belonging to the acenes series by using density functional theory combined with the non-equilibrium Green's function approach to electronic transport. While short acenes are found to be non-magnetic, molecules comprising more than nine acene rings have a spin-polarized ground state. In their gas phase these have a singlet total spin configuration, since the two unpaired electrons occupying the doubly degenerate highest molecular orbital are antiferromagnetically coupled to each other. Such an orbital degeneracy is however lifted once the molecule is attached asymmetrically to Au electrodes via thiol linkers, leading to a fractional magnetic moment. In this situation the system Au/ n -acene/Au can act as an efficient spin-filter with interesting applications in the emerging field of organic spintronics.

PACS numbers: 75.76, 85.75, 72.25

1. Introduction

Molecules of the n -Acenes family, $C_{4n+2}H_{2n+4}$, are an important class of organic compounds formed from polycyclic aromatic hydrocarbons consisting of linearly fused benzene rings. These molecules, schematically shown in figure 1, can be also viewed as small hydrogen terminated graphene nano-ribbons. The interest in their electronic properties has grown enormously in the past few years [1–24]. The smallest acenes, benzene ($n = 1$) and naphthalene ($n = 2$), are well known aromatic compounds, while the intermediate ones, tetracene ($n = 4$) and pentacene ($n = 5$), are semiconductor materials in their solid phase. These are commonly used in organic field effect transistors [5,25], organic light emitting diodes [26,27] and organic photovoltaic cells [28], because of their high charge carrier mobility. For pentacene single crystals a value of $35 \text{ cm}^2\text{V}^{-1}\text{s}^{-1}$ was reported [17], which is among the highest mobility of all organic semiconductors. As we move to still larger acenes, which we will refer here to as higher acenes, such as heptacene ($n = 7$), octacene ($n = 8$), nonacene ($n = 9$) and decacene ($n = 10$), the structural stability is reduced. Those molecules are in fact quite reactive and the experimental literature become less rich.

Theoretical studies predict that the higher acenes are good candidates for realizing p -type magnetism, i.e. magnetism without ions presenting partially filled d or f shells [7–12]. If the larger magnetic acenes can be stabilized, their magnetism coupled with the long spin-diffusion length will make this material class extremely appealing for the next generation of organic spintronics devices [29–33].

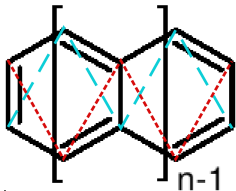


Figure 1. (Colour on line) Schematic illustration of the n -Acene series. The dashed (light blue) and dotted (red) line denote the symmetry of the two degenerate HOMOs.

The smaller acenes have a non-magnetic (diamagnetic) ground state. For the higher acenes calculations predict the edges of the molecule to be spin polarized [7–9,11,12,18]. In this case there are two degenerate highest occupied molecular orbitals (HOMOs), each of them populated by a single electron. One of the HOMOs is localized mainly on the hydrogenated carbon atoms at one edge of the molecule, while the other HOMO is localized on the opposite edge. These two degenerate molecular orbitals extend in a zigzag-like symmetry along the length of the molecule as indicated by the dashed lines in Fig 1. These states are similar in nature to the edge states found in graphene nano-ribbons [34]. The lowest unoccupied molecular orbitals (LUMOs) are the corresponding empty spin-split orbitals, so that the HOMO-LUMO gap is an

exchange split gap. Recent calculations predicted a spin singlet ground state for the higher acenes [7, 8, 11, 12, 18] as a result of the antiferromagnetic coupling between the two orbitally degenerate HOMOs. This contrasts earlier predictions of a ferromagnetic (triplet) ground state [10, 19, 20].

Since small acenes are diamagnetic and the higher ones are predicted magnetic, there is a critical length for the onset of magnetism. This is generally accepted to occur for n between 6 and 8, but there is no consensus on the precise value. Houk *et al.* [10] used the B3LYP functional and found that for more than 8 acene rings a triplet ground state is lowest in energy. Bendikov *et al.* [7, 8] performed calculations at the UB3LYP level and observed a magnetic ground state already for 6 acene rings. Finally Jiang *et al.* [12] found the transition to a magnetic ground state for more than 7 benzene rings.

From the experimental point of view, a significant amount of work has been devoted to the study of electron transport through pentacene [21–24]. The same material has also been used as a medium for spin-polarized transport in composite junctions [35] with some evidence for spin-injection [36]. Pentacene itself however is not magnetic. For this reason significant new effort is being made to synthesize the higher acenes [1–6, 14, 16]. After much skepticism about its stability [15], heptacene was finally synthesized in 2006, and subsequent analysis has shown that the ground state is non magnetic [3, 16]. More recently Tonshoff and Bettinger synthesized octacene and nonacene [6], and importantly there is spectroscopical evidence for anti-ferromagnetism in nonacene [6].

In this work we investigate both the ground state electronic structure and the electronic transport properties of the higher acenes. In particular we focus our attention on pentacene and decacene, in order to compare results for a non-magnetic molecule, such as pentacene, to those of a magnetic one, such as decacene.

2. Methods

The electronic structure is calculated by using spin polarized density functional theory (DFT), as implemented in the SIESTA code [37]. The transport properties are then obtained with the non-equilibrium Green’s function (NEGF) code SMEAGOL [38–40], which shares the Kohn-Sham Hamiltonian with SIESTA. The LDA functional [42] is used throughout this work. A double- ζ (DZ) basis was used to describe the electronic structure of the valence electrons of the molecule, while we use an s only single- ζ basis set for the gold electrodes. This has been extensively tested in the past [43, 44] and offers a good compromise between accuracy and computational demands. A real space grid with an equivalent plane wave cutoff of 300 Ry is used to sample the electronic density. For the isolated molecule periodic images are separated by a minimum of 10 Å, which is found to be sufficient to prevent interaction between the image molecules. For all the molecules structural relaxation is performed by standard conjugate gradient to a force tolerance of 0.01 eV/Å.

The transport junction is constructed by connecting the molecules to a Au fcc (111) surface via sulfur anchoring groups with a S-Au bond length of 1.9 Å [41]. We use a

k -point mesh with a cutoff of 9 Å perpendicular to the transport direction. Due to the presence of many local minima, which are found for the different local magnetic alignments, it was necessary to initialize the calculations with several different spin configurations for both the electronic structure and the transport calculations in order to ascertain the global ground state.

3. Results

3.1. Electronic structure of n -Acene molecules: gas phase

We calculate the electronic structure of the isolated n -acenes for the molecules of different lengths ranging from 5 acene rings ($n = 5$, pentacene) up to 10 ($n = 10$, decacene). A non magnetic ground state is found for $n \leq 8$, whereas nonacene and decacene present a spin polarized ground state. For these the atoms at the upper and lower edges of the molecules have an equal and opposite magnetic moment, corresponding to an anti-ferromagnetic local spin arrangement (see figure 2). This is consistent with previous results on higher acenes [7,12], and it is similar to the edge-state magnetism predicted for graphene nano-ribbons [34]. In decacene the total energy for the anti-ferromagnetic phase is $\Delta E = 40$ meV smaller than that of the ferromagnetic one and $\Delta E = 110$ meV smaller than that of a non-spin polarized solution.

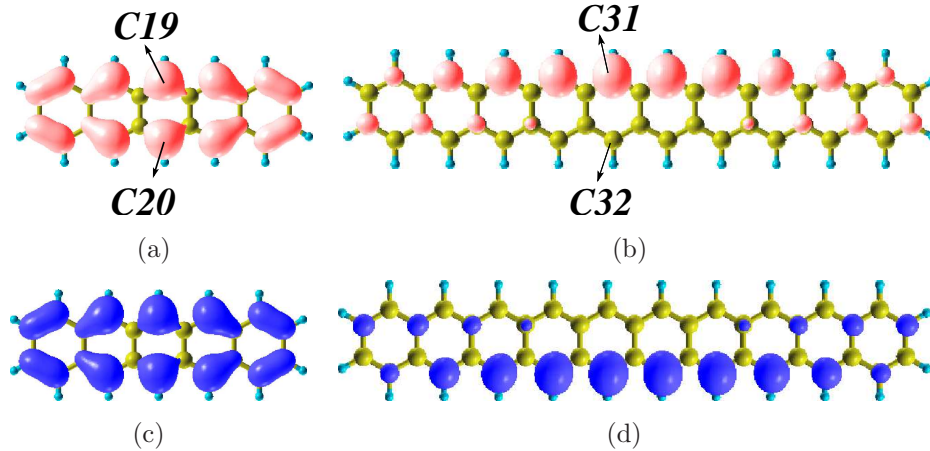


Figure 2. (Colour on line) Spin-resolved electron density of the HOMO of both pentacene and decacene. The various panels are respectively for: (a) pentacene majority spins, (b) decacene majority spins, (c) pentacene minority spins, (d) decacene minority spins. In the molecule structure the large light grey (yellow) spheres are for C and the small grey (light blue) ones are H.

The total spin-resolved density of states (DOS) projected over all the carbon atoms is shown in figure 3(a) for pentacene and in figure 3(b) for decacene. In both cases there is no net spin-polarization. However, while for pentacene all the molecular orbitals are spin-degenerate, in decacene spin-symmetry is locally lifted. This can be appreciated by looking at the projected density of states (PDOS) on the two carbons atoms located

in the middle of molecules at opposite edges [in the case of decacene these are the atoms labelled as C31 and C32 in figure 2(b)]. The PDOS are shown in figure 3(c) and 3(d) for pentacene and decacene, respectively. It is then clear that for decacene the majority spins are located on the upper edge, while the minority ones on the lower edge. This means that, although decacene does not provide a net spin polarization over the entire molecule, it is locally magnetic. It is then expected that a net magnetic moment can be created by breaking the molecule axial symmetry. In the following sections we will demonstrate that this can indeed be achieved when attaching the molecule asymmetrically to metallic electrodes.

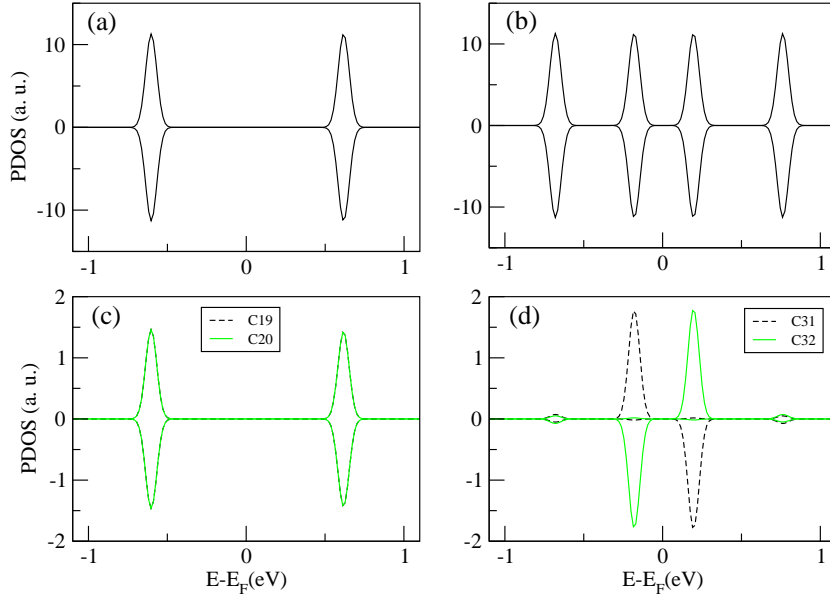


Figure 3. Projected density of states (PDOS) over selected atoms: (a) all the C atoms of pentacene, (b) all the C atoms of decacene, (c) middle two C atoms of pentacene, (d) middle two C atoms of decacene. Positive PDOS are for the majority spins and the negative are for the minority.

We then calculate the HOMO-LUMO gap for all the acenes ranging from pentacene to decacene (see figure 4). As the number of benzene rings increases, the HOMO-LUMO gap is reduced. Interestingly the dependence of the HOMO-LUMO gap on the acene length changes as $n > 8$, i.e. as the molecules develop a spin-polarized ground state. In fact for the magnetic molecule the gap is an exchange gap between the spin split molecular orbitals with the same orbital symmetry. Such an exchange gap is not strongly length dependent and it is expected to saturate to a constant value characteristic of the infinite graphene ribbon. Finally we note that, if a non-magnetic solution is forced one will expect a gap closure for sufficiently long molecules.

It is important to remark at this point that the limitations of the LDA exchange correlation functional make our calculated HOMO-LUMO gap smaller than the experimental one. The experimental gap of pentacene in the gas phase is found to be 5.54 eV [45], whereas our calculations report a value of only about 1.2 eV. Certainly one

should not expect the Kohn-Sham HOMO-LUMO gap to reproduce the true excitation gap of the molecule. Still in the NEGF scheme the Kohn-Sham eigenvalues are effectively used as single particle levels for the transport, and one should then ask whether the LDA description is sufficient [46]. Notably when a molecule is attached to a metallic surface its ionization potential (IP) is usually reduced due to large correlation effects. In [47] the HOMO-LUMO gap of pentacene on graphite is calculated by the GW method to be about 2.88 eV. We therefore expect that our LDA HOMO-LUMO gap for pentacene on the surface is underestimated by about a factor 2 with respect to experiments. In fact, experimental data [48] return a HOMO-LUMO gap of about 2.2 eV for pentacene thin films on Au. There are no experimental data on the decacene IP, however we expect a deviation from experiments similar to the one of pentacene.

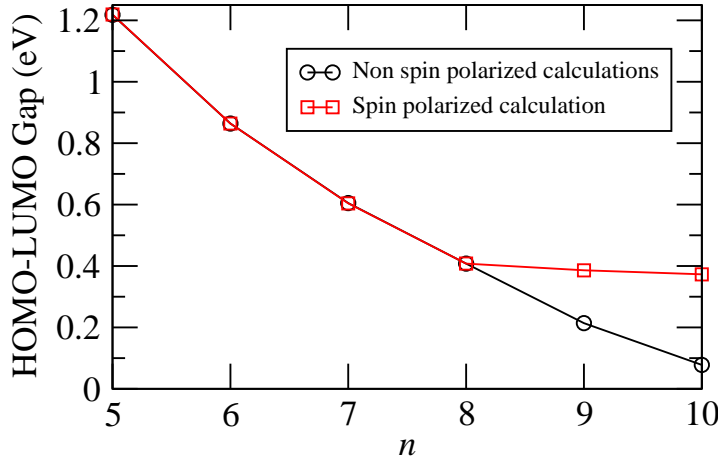


Figure 4. HOMO-LUMO gap calculated from the Kohn-Sham eigenvalues for n -acenes as a function of n .

3.2. Transport properties

We now investigate the electronic structure and the transport properties of the molecules attached to Au electrodes. We use thiol groups to bind the acenes to the Au surface and consider four different binding geometries. These are shown for decacene in figure 5. Panel (a) shows the meta configuration, in which only the two ends of the lower edge are connected to Au. figure 5(b) shows the para configuration, where the lower edge on the left side and the upper edge on the right side are connected to the electrodes. figure 5(c) corresponds to the meta configuration with an additional S linker on the left side upper edge, and in figure 5(d) there are 4 S linkers.

The ground state of the isolated thiolated molecules is anti-ferromagnetic for decacene, and non-magnetic for pentacene. This demonstrates that the electronic structure of the isolated molecules is affected little by the attachment of the S-H end-groups. We typically run multiple simulations for each geometries by initializing the density matrix in different spin states. In the case of the complete junction (electrodes

plus molecule) we find always an identical final spin configuration regardless of the initialization, so that any other metastable solution cannot be stabilized during the self-consistent cycle. In particular the calculations for pentacene all converge to a non-magnetic solution, while those for decacene to a spin-polarized one. In this second case the coupling to the electrodes determines the final magnetic state.

When the coupling is asymmetric [figures 5(a) and 5(c)] the system develops a significant fractional magnetic moment, while no moment is found for the symmetric geometries [figures 5(b) and 5(d)]. In general the coupling to the electrodes leads to level broadening and consequently to charge transfer from the molecule HOMO to the Au. Thus, whereas the majority HOMO is always fully filled, the minority one may have partial occupation and the total spin-polarization may be non-zero. The fact that different density matrix initializations result in the same solution indicates that, at variance with the isolated molecule which possess different local energy minima corresponding to different magnetic states, when the molecule is attached to Au there is only one robust global minimum. For the meta configuration the energy of this single global minimum is about 100 meV smaller than that of the non-spin polarized solution. figure 5 shows the isosurfaces associated to the spin-density (the charge density difference

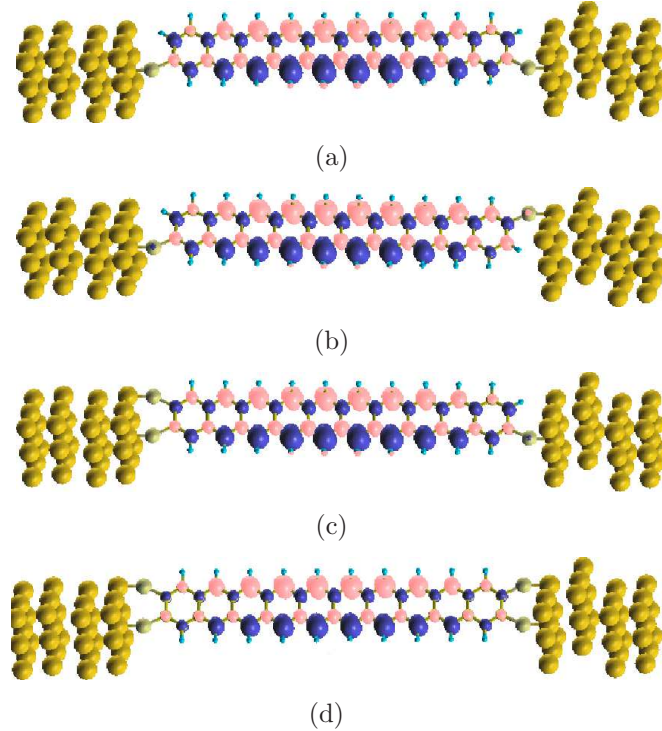


Figure 5. (Colour on line) Isosurfaces of spin density magnetization for the various anchoring geometry of decacene attached to Au via a thiol group: a) two links, meta; b) two links, para; c) three links d) four links. Positive isosurfaces are represented in light grey (pink) and negative ones in dark grey (blue).

between majority and minority spins) of decacene for the four geometries investigated. From the figure, one can notice the general antiferromagnetic coupling between the spins

of the two edge states, a characteristic feature of the molecule in its gas phase, which is largely preserved when the molecular junction is made. The coupling to the electrodes in some cases breaks the axial symmetry of the molecule and a magnetic moment arises. This is $0.54 \mu_B$ for the meta configuration [figure 5(a)] and $0.32 \mu_B$ for the structure of figure 5(c). No moment is then found for the two symmetric configurations [figure 5(b) and figure 5(d)].

In order to analyze the effect of the different linking geometries on the electronic structure and the transport properties of the junctions, we calculate for all the configurations the DOS projected on the central C atoms of decacene (figure 6), and the zero-bias transmission coefficient (figure 7). Note that in figure 6 we use no additional broadening, so that the width of the DOS peaks is caused entirely by their coupling to the Au electrodes. For the meta configuration [figure 6(a)] the broadening of the DOS

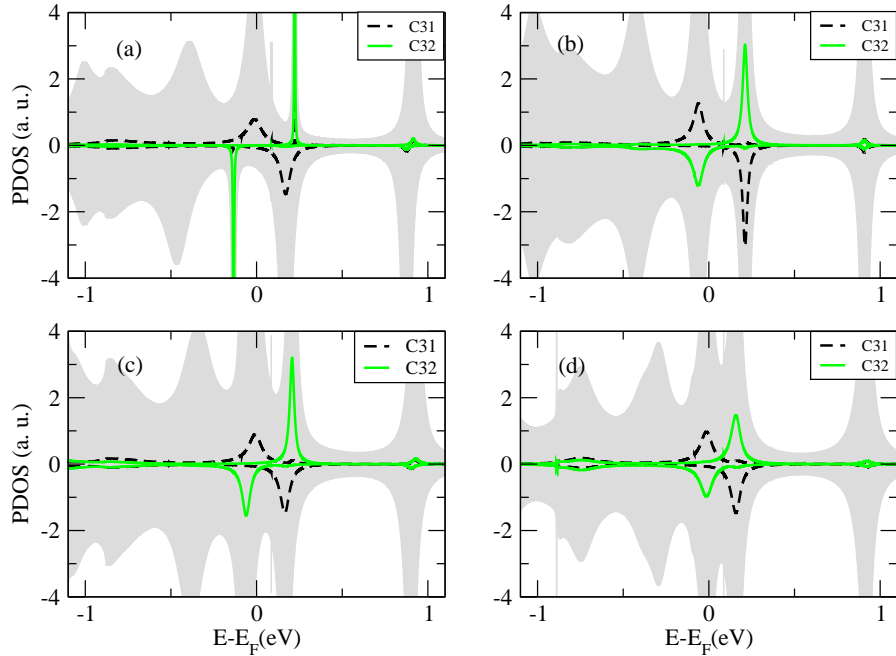


Figure 6. PDOS for two carbons atom in the middle of decacene molecule (C31 and C32) for different anchoring configurations: a) two links, meta; b) two links, para; c) three links d) four links. The grey shadow is the total DOS of the molecule.

for states located on the upper edge of the molecule (atom C31) is larger than that of the states located on the lower edge (atom C32). This indicates strong coupling for the upper edge state and weak coupling, i.e. stronger localization, for the lower one, as expected from the bonding geometry. The spin-splitting of the states with higher coupling to the Au electrodes is reduced from its value for decacene in the gas phase. Furthermore a strong electron coupling enhances the partial charge transfer from the Au electrodes, so that the strongly coupled edge state is closer to the Fermi energy (E_F) for both the HOMO and LUMO. Consequently the zero-bias transmission [figure 7(a)] for majority and minority spins is different. Intriguingly, at E_F the transmission coefficient

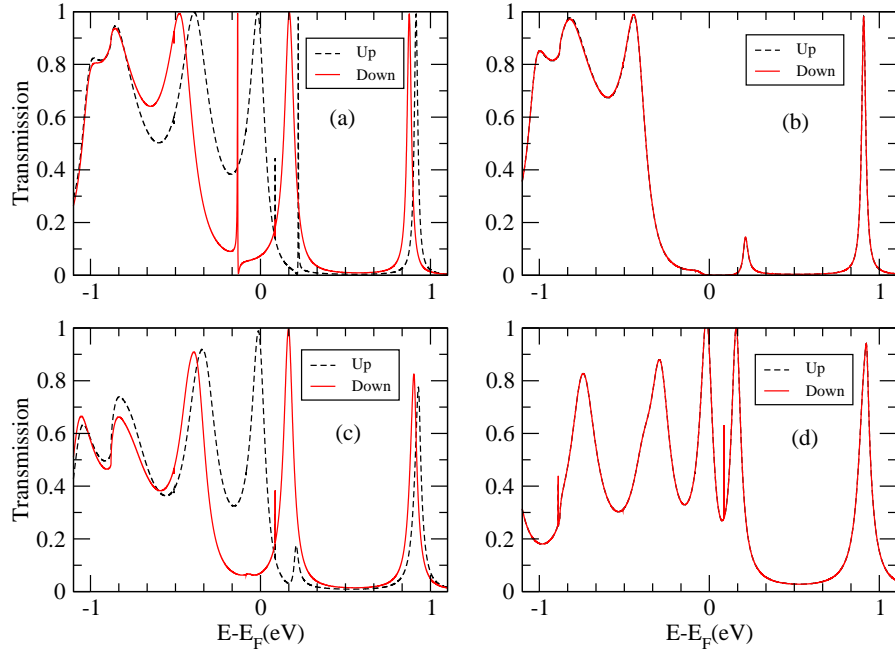


Figure 7. Transmission coefficient for decacene for the different anchoring configurations: a) two links, meta; b) two links, para; c) three links d) four links. Up and Down indicate respectively the majority and minority spins contributions.

for majority electrons is much larger than that for the minority ones, so that we expect a large spin-polarization of the current at small biases. This demonstrates that it is possible to obtain a spin-polarized current in n -acenes without using magnetic leads by simply exploiting their intrinsic magnetic nature and by engineering an asymmetric bonding to a metallic surface.

In the para configuration [figure 5(b)] majority and minority states have the same coupling strength to the electrodes, since the two edges of the molecule are identically coupled. The PDOS [figure 6(b)] associated to the two edges is symmetric and consequently no spin polarization is seen in the transmission coefficient of figure 7(b). Then, when the molecule is anchored to Au through three links [figure 5(c)], although the minority spin density is not as localized as in the meta configuration, it is still more localized than the majority spin density. As such also here the electron transmission is different transmission for the two spins directions. Finally, when the molecule is connected to both the edges with a total of 4 thiol groups we recover the complete symmetry between the two edges, and therefore the non-spin polarized transmission [see figures 6(d) and 7(b)]. The coupling strength to the electrodes can be quantitatively described as indicated in [43]. In brief, one can approximate the transmission coefficient as a function of energy, $T_\alpha(E)$, around a particular molecular orbital with energy ϵ_α with a Breit-Wigner-like expression

$$T_\alpha(E) = \frac{\gamma_\alpha^L \gamma_\alpha^R}{(E - \epsilon_\alpha)^2 + (\gamma_\alpha/2)^2}.$$

Here γ_α^L (γ_α^R) is the coupling strength of that particular molecular orbital with the left-hand side (right-hand side) electrode. As such the full width at half maximum (FWHM) of a peak in the transmission coefficient is $\text{FWHM} = \gamma_\alpha = \gamma_\alpha^L + \gamma_\alpha^R$. For symmetric coupling to the electrodes we have $\gamma_\alpha^L = \gamma_\alpha^R = \text{FWHM}/2$. Note that the same level broadening is found for the DOS and that this can be directly extracted from the NEGF density matrix.

Let us focus as an example on the meta configuration. In this case the majority spin levels, localized on the upper edge of the molecule, are coupled to the electrodes via the thiol group. In contrast the minority spin levels, localized on the lower edge, can be accessed from the electrodes only through tunneling in vacuum, since there is no direct binding atom. We then calculate a FWHM for the majority HOMO and LUMO respectively of 100 meV and 67 meV. Although minor differences in the orbital wavefunction produce differences in the FWHM we conclude that the overall coupling of the upper edge levels is of the order of $\gamma_\alpha = 84$ meV, which corresponds to a life-time of 5 ps. The same analysis carried out for the minority spins gives us $\gamma_\alpha = 2$ meV and a life-time of 200 ps. We then conclude that the electronic coupling of the thiolated edge is approximately 40 times stronger than that of the non-thiolated one.

We now briefly discuss the potential consequences arising from the LDA underestimation of the HOMO-LUMO gap. In general the main drawback is that both the HOMO and the LUMO are artificially too close to the electrodes E_F . Therefore the calculated charge transfer from the molecule majority HOMO to Au is likely to be overestimated. As a consequence also the net magnetic moment is probably overestimated. If one assumes that the charge transfer is negligible at zero-bias then the total magnetic moment will be close to zero. However even in such a situation a charge transfer and consequently a net magnetic moment can originate either at finite bias or by applying an electrostatic gate to the molecules. Therefore the finding of a total magnetic moment on the molecule is a general feature of such an interface, since it depends entirely on the fact that there is a considerably different electronic coupling to Au for the two spin channels of the molecule. The fact that such a magnetic moment that can be potentially tuned via bias or gate voltage opens intriguing possibilities for device applications.

In order to compare results for molecules of different length, we performed additional calculations for the Au/ n -acene/Au junction in the meta configuration and for different n . In general we find spin-polarized transmission for molecules made up of more than 8 rings (see figure 8 for the magnetic moment of the junction as a function of n). The features of these magnetic molecule junctions are qualitatively similar to those described in details for decacene. For the sake of comparison in figure 9 we present the PDOS and the zero-bias transmission for a representative non-magnetic acene, namely pentacene. Since the ground state is non-magnetic the PDOS of the carbon atoms on the upper edge is the same as that on the lower edge. Therefore we find a completely non spin-polarized zero-bias transmission [see figure 9(b)]. Importantly transport measurements for pentacene on Au indicate hole conductance [17]. This is

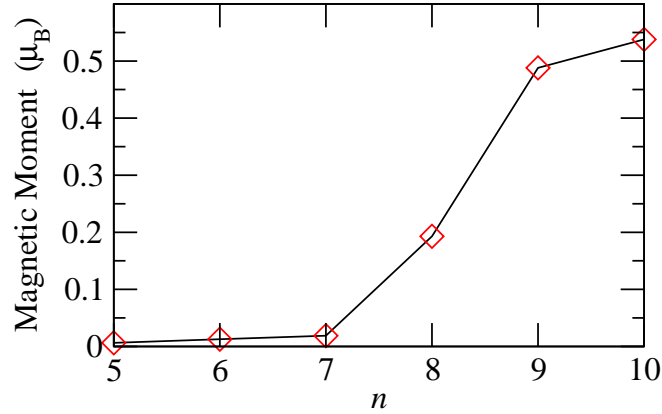


Figure 8. Magnetic moment of the Au/ n -acene/Au junction as a function of the molecule length, n .

consistent with our results, which do indicate HOMO transport. However due to the underestimated IP our low bias conductance is likely to be overestimated.

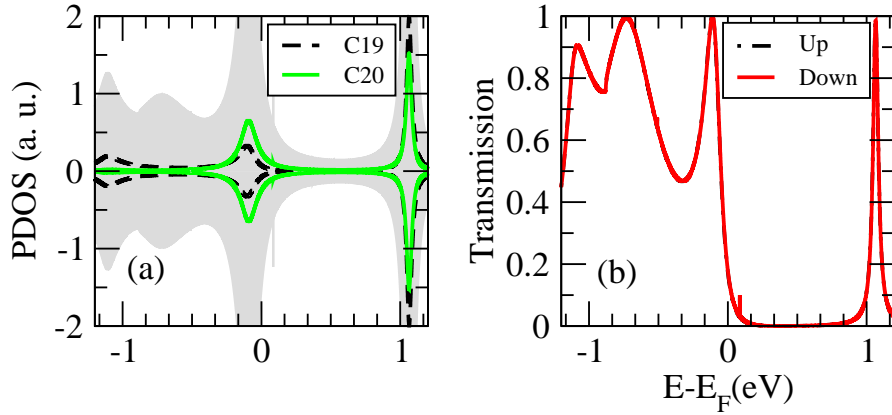


Figure 9. Projected density of states (a) and transmission coefficient (b) for pentacene in the meta anchoring configuration.

4. Conclusions

We have examined the electronic structure and spin transport properties of higher acenes molecules attached to Au electrodes. These have been compared with those of the smaller members of the acene family. We find that the isolated molecules have a spin-polarized ground state for molecules containing more than 8 acene rings. However the total moment vanishes even for the magnetic acenes, since the electrons in the two degenerate HOMO levels couple anti-ferromagnetically to each other. These results are in good agreement with both previous calculations and with the most recent experimental evidence. When such molecules are attached to Au via thiol linkers, a transition from a non-magnetic to a magnetic ground state occurs at 8 acene rings.

The coupling between the two HOMO levels is still found to be anti-ferromagnetic. However, when the electronic interaction of the molecule with the electrodes is different between the two molecule edges than fractional charge transfer leads to a total net spin. The Au/*n*-acene/Au system acts then as a spin filter. Such a spin-filtering property can be achieved by binding the molecule to Au via thiol linkers in an asymmetric way. We finally speculate on the fact that the charging state of the molecule and hence its magnetic moment can be controlled by bias and/or electrostatic gating.

Acknowledgments

IR, TA and SS acknowledge financial support from Science foundation of Ireland (07/IN.1/I945 and No. 07/RFP/PHYF235), CRANN and the EU FP7 project ATHENA. Computational resources have been provided by the HEA IITAC project managed by TCHPC and by ICHEC.

References

- [1] Chun D, Cheng Y and Wudl F 2008 *Angew. Chem.* **120** 8508
- [2] Kaur I, Jazdzzyk M, Stein N N, Prusevich P and Miller G P 2010 *J. Am. Chem. Soc.* **132** 1261
- [3] Mondal R, Shah B K and Neckers D C 2006 *J. Am. Chem. Soc.* **128** 9612
- [4] Payne M M, Parkin S R and Anthony J E 2005 *J. Am. Chem. Soc.* **127** 8028
- [5] Anthony J 2008 *Angew. Chem. Int. Ed.* **47** 452
- [6] Tonshoff C and Bettinger H F 2010 *Angew. Chem. Int. Ed.* **49** 4125
- [7] Bendikov J M, Duong H M, Starkey K, Houk K N, Carter E A and Wudl F 2004 *J. Am. Chem. Soc.* **126** 7416
- [8] Bendikov J M, Duong H M, Starkey K, Houk K N, Carter E A and Wudl F 2004 *J. Am. Chem. Soc.* **126** 10493
- [9] Dos Santos M C 2006 *Phys. Rev. B* **74** 045426
- [10] Houk K N, Lee P S and Nendel M 2001 *J. Org. Chem.* **66** 5107
- [11] Hachmann J, Dorando J J, Aviles M and Chan G K 2007 *J. Chem. Phys.* **127**, 134309
- [12] Jiang D and Dai S 2008 *J. Phys. Chem. A* **112** 332
- [13] Hajgat6 B, Szieberth D, Geerlings P, Proft F D and Deleuze M S 2009 *J. Chem. Phys.* **131** 224321
- [14] Zade S S and Bendikov M 2010 *Angew. Chem. Int. Ed.* **49** 4012
- [15] Clar E 1964 *Polycyclic Hydrocarbons* vol 1 (New York: Academic Press)
- [16] Bettinger H F, Mondal R and Neckers D C 2007 *Chem. Commun.* 5209
- [17] Jurchescu O D, Baas J and Palstra T T M 2004 *Appl. Phys. Lett.* **84** 3061
- [18] Qu Z, Zhang D, Liu C and Jiang Y 2009 *J. Phys. Chem. A* **113** 7909
- [19] Angliker H, Rommel E and Wirz J 1982 *Chem. Phys. Lett.* **87** 208
- [20] Nijegorodov N, Ramachandran V and Winkoun D P 1997 *Spectrochim. Acta A* **53** 1813
- [21] Puigdollers J, Voz C, Martin I, Orpella A, Vetter M and Alcubilla R 2004 *Journal of Non-Crystalline Solids* **338-340** 617
- [22] Yanagisawa H, Tamaki T, Nakamura M and Kudo K 2004 *Thin Solid Films* **464-465** 398
- [23] ElAmrani A, Lucas B and Moliton A 2008 *Eur. Phys. J. Appl. Phys.* **41** 19
- [24] Diao L, Frisbiea C D, Schroepfer D D and Ruden P P 2007 *J. Appl. Phys.* **101** 014510
- [25] Park S K, Jackson T N, Antony J E and Mourey D A 2007 *Appl. Phys. Lett.* **91** 063514
- [26] Jang B B, Lee S H and Kafafi Z H 2006 *Chem. Mater* **18** 499
- [27] Wolak M A, Jang B B, Palilis L C and Kafafi Z H 2004 *J. Phys. Chem. B* **108** 5492
- [28] Rand B P, Genoe J, Heremans P and Poortmans J 2007 *J. Prog. Photovoltaics* **15** 659

- [29] Sanvito S 2007 *J. Mat. Chem.* 2007 **17** 4455
- [30] Sanvito S 2007 *Nature Materials* **6** 803
- [31] Dediu V A, Hueso L E, Bergenti I and Taliani C 2009 *Nature Materials* **8** 707
- [32] Bogani L and Wernsdorfer W 2008 *Nature Materials* **7** 179
- [33] Szulczewski G, Sanvito S and Coey J M D 2009 *Nature Materials* **8** 693
- [34] Zheng X H, Rungger I, Zeng Z and Sanvito S 2009 *Phys. Rev. B* **80** 235426
- [35] Shimada T, Nogawa H, Noguchi T, Furubayashi Y, Yamamoto Y, Hirose Y, Hitosugi T and Hasegawa T 2008 *Jpn. J. Appl. Phys.* **47** 1184
- [36] Ikegami T, Kawayama I, Tonouchi M, Nakao S, Yamashita Y and Tada H 2008 *Appl. Phys. Lett.* **92** 153304
- [37] Soler J M, Artacho E, Gale J D, Garcia A, Junquera J, Ordejón P and Sanchez-Portal D 2002 *J. Phys. Condens. Matter* **14** 2745
- [38] Rocha A R, Garcia-Suarez V M, Bailey S W, Lambert C J, Ferrer J and Sanvito S 2005 *Nature Mater* **4** 335
- [39] Rocha A R, Garcia-Suarez V M, Bailey S W, Lambert C J, Ferrer J and Sanvito S 2006 *Phys. Rev. B* **73** 085414
- [40] Rungger I and Sanvito S 2008 *Phys. Rev. B* **78** 035407
- [41] Toher C, Rungger I and Sanvito S 2009 *Phys. Rev. B* **79** 205427
- [42] Perdew J P and Zunger A 1981 *Phys. Rev. B* **23** 5075
- [43] Pemmaraju C D, Rungger I and Sanvito S 2009 *Phys. Rev. B* **80** 104422
- [44] Rungger I, Chen X, Schwingenschlögl U and Sanvito S 2010 *Phys. Rev. B* **81** 235407
- [45] Dolomatov M Yu and Mukaeva G R 1991 *J. Appl. Spectroscopy* **53** 1286
- [46] Toher C, Filippetti A, Sanvito S and Burke K 2005 *Phys. Rev. Lett.* **95** 146402
- [47] Neaton J B, Hybertsen M S and Louie S G 2006 *Phys. Rev. Lett.* **97** 216405
- [48] Koch N, Kahn A, Ghijsen J, Pireaux J J, Schwartz J, Johnson R L and Elschner A 2003 *Appl. Phys. Lett.* **82** 70